Centrality determination with HADES

HADES

Abstract The centrality determination for Au+Au collisions at 1.23A GeV, as measured with HADES at the GSI-SIS18 is described. In order to extract collision geometry related quantities, such as the average impact parameter or number of participating nucleons, a Glauber Monte Carlo approach is employed. For the application of this model to collisions at this relatively low centre-of-mass energy special investigations had to be done, whose details are summarized here.

1 Introduction

Heavy-ion collisions at high energies allow to study highly compressed strongly interacting matter. Due to the extended volume of the colliding nuclei, the size of the interaction volume varies strongly with impact parameter b, defined as the distance between the centres of the nuclei in a plane transverse to the beam axis. Therefore, it is crucial to define a framework which allows to relate observable quantities, such as the measured charge particle multiplicity, to the centrality of the collision. The centrality C is expressed as the fraction of the total cross section and is directly related to the impact parameter:

$$C = \frac{\int_0^b d\sigma/db' \, db'}{\int_0^\infty d\sigma/db' \, db'} = \frac{1}{\sigma_{AA}} \int_0^b \frac{d\sigma}{db'} \, db' \; . \quad (1)$$

Experiments at higher energies usually employ the Glauber model [1–3] for this purpose, as described e.g. in Refs. [4, 5]. In this approach, heavy-ion collisions are treated as a superposition of independent nucleon-nucleon interactions. Following the eikonal approximation, the trajectories of the individual nucleons are assumed to be straight lines and a nucleon is defined as a participant, if it experiences at least
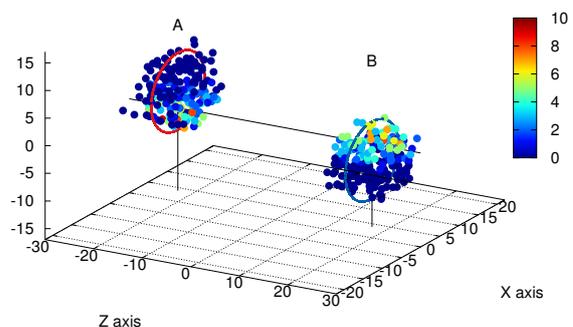
Fig. 1 Spatial distribution of the nucleons of two colliding nuclei A and B as generated with the Glauber MC model. The beam direction is along the Z-axis. The color scheme encodes the number of collisions that a single nucleon experiences in this particular collision process.

one binary collision along its path. The number of participating nucleons $N_{\rm part}$ can thus be used to quantify the size of the interaction volume. The number of spectators, i.e. of non-interacting nucleons, is related to the participants by $N_{\rm spec} = A_{\rm proj} + A_{\rm targ} - N_{\rm part}$, where $A_{\rm proj}$ ($A_{\rm targ}$) is the atomic number of the projectile (target) nucleus. Following the assumptions of the wounded nucleon model [6], the number of produced particles should be directly proportional to $N_{\rm part}$. This relation thus allows to fit measured multiplicity distributions with a Glauber Monte Carlo model, in which many nucleus-nucleus collisions are statistically sampled. Based on this fit, centrality classes with their corresponding average impact parameter $\langle b \rangle$ and number of participants $\langle N_{\rm part} \rangle$ can be derived by selecting intervals of event multiplicity.

While the validity of the Glauber model at higher energies (i.e. $\sqrt{s_{\rm NN}}$ around 10 GeV and above) is well estab-

lished, the applicability at lower energies is not immediately clear. The semi-classical description of the eikonal approximation requires that the reduced de Broglie wavelength, $\lambdabar_B = \hbar/p$, where p is the characteristic momentum of the particle, is small relative to the size of the nucleus. This condition is clearly satisfied for a nucleon of ~ 2 GeV$/c$ momentum traversing a gold nucleus at rest, a situation close to Au+Au collisions at 1.23A GeV:

$$\lambdabar_B \approx 0.2 \text{ fm} \ll R \approx 5.4 \text{ fm}. \tag{2}$$

Indeed, it was shown that with appropriate corrections of the order of 15 % the validity of the eikonal Glauber Model can even be extended down to energies as low as about 45 MeV [7]. In this article, we describe the application of a Glauber MC model to Au+Au data at 1.23A GeV, as measured with HADES[1], which is positioned at the SIS18[2] accelerator at the GSI[3] in Darmstadt, Germany. The implementation and the adjustments to the model, necessary for this data set, are discussed and the experimental observables for the charged particle multiplicity as used for the centrality determination are presented.

2 Glauber MC model implementation

The analysis discussed in the following is based on the implementation of a Glauber MC model as described in Refs. [4, 8]. In this MC approach the following steps are processed event-by-event:

1. The impact parameter b of a given collision is selected randomly according to a probability distribution $P(b) \propto b \, db$ in the range from 0 to $b_{\max}$, where $b_{\max}$ has to be larger than the sum of the radii of the projectile and target nucleus, $b_{\max} \geq R_{\text{proj}} + R_{\text{targ}}$.
2. For each of the nuclei, the N_{proj} and N_{targ} nucleons are positioned randomly. This is achieved by using a uniform probability distribution in the azimuthal ($\cos\theta$) and polar (ϕ) angles, and a radial density distribution given by $P(r) \propto r^2 \rho(r)$.
3. The collision process itself is evaluated such that binary combinations of all nucleons in the two nuclei are formed and a decision is made whether a collision is actually taking place between them. This decision is based on the criterion that the distance between nucleon i and j in the transverse plane, $d_{ij} = \sqrt{\Delta x^2 + \Delta y^2}$, is smaller than the radius defined by the inelastic nucleon-nucleon cross section (black disk approximation):

$$d_{ij}^2 \leq \sigma_{\text{inel}}^{\text{NN}}/\pi \tag{3}$$

---

[1] High-Acceptance Di-Electron Spectrometer
[2] Schwer-Ionen-Synchrotron
[3] Gesellschaft für Schwerionenforschung

Figure 1 shows an example for the spatial configuration of two colliding nuclei obtained with the above described procedure. In order to apply the Glauber MC model to the relatively low centre-of-mass energies of the heavy-ion collisions under consideration here, several adjustments had to be performed [9]. To parametrize the radial charge density distributions a two-parameter Fermi distribution was used:

$$\rho(r) = \frac{1 + w\,(r/R)^2}{1 + \exp\left(\frac{r-R}{a}\right)} \tag{4}$$

For the Au-nuclei we use the parameters $R = 6.55$ fm and $a = 0.52$ fm, which best describe the measurements in [10]. The parameter w, which is used to describe nuclei whose density is lower at the centre than in the outer regions, is here set to $w = 0$. To make sure that two nucleons cannot overlap in space, a new position can be reassigned to one of them during step (ii) of the MC procedure, if their distance falls below a minimal separation distance $d_{\min}$. This is of particular importance if the Glauber MC model is used to investigate eccentricities in the nucleon configuration which are affected by spatial correlations between the nuclei. As value for this inter-nucleon exclusion distance $d_{\min} = 0.9$ fm is used. While at high energies the inelastic nucleon-nucleon cross section is only weakly dependent on $\sqrt{s_{\text{NN}}}$, it exhibits a rapid variation with energy in the energy regime discussed here. Possible variations thus constitute a significant contribution to the systematic uncertainty (see Sect. 4.1). Based on the data collected in [11] and parametrized by [12] we use the following values as default: $\sigma_{\text{inel}}^{\text{pp}} = 26.4$ mb and $\sigma_{\text{inel}}^{\text{np}} = 21.0$ mb. Assuming isospin symmetry (i.e. $\sigma_{\text{inel}}^{\text{pp}} = \sigma_{\text{inel}}^{\text{nn}}$ and $\sigma_{\text{inel}}^{\text{np}} = \sigma_{\text{inel}}^{\text{pn}}$), we construct the isospin averaged nucleon-nucleon cross section for an Au-nucleus as $\sigma_{\text{inel}}^{\text{NN}} = 23.8$ mb.

3 Experimental observables

The setup of the HADES experiment is described in detail in [13]. HADES is a charged particle detector consisting of a six-coil toroidal magnet centered around the beam axis and six identical detection sections located between the coils and covering polar angles between $18°$ and $85°$. Each sector is equipped with a Ring-Imaging Cherenkov (RICH) detector followed by four layers of Multi-Wire Drift Chambers (MDCs), two in front of and two behind the magnetic field, as well as a scintillator Time-Of-Flight detector (TOF) ($45° - 85°$) and Resistive Plate Chambers (RPC) ($18° - 45°$). Hadron identification is based on the time-of-flight measured with TOF and RPC, and on the energy-loss information from TOF as well as from the MDC tracking chambers. Electron candidates are in addition selected via their signals in the RICH detector. Combining these information with the track momenta, as determined from the change of the track direction in the magnetic field, allows to identify all stable particles with high significance.
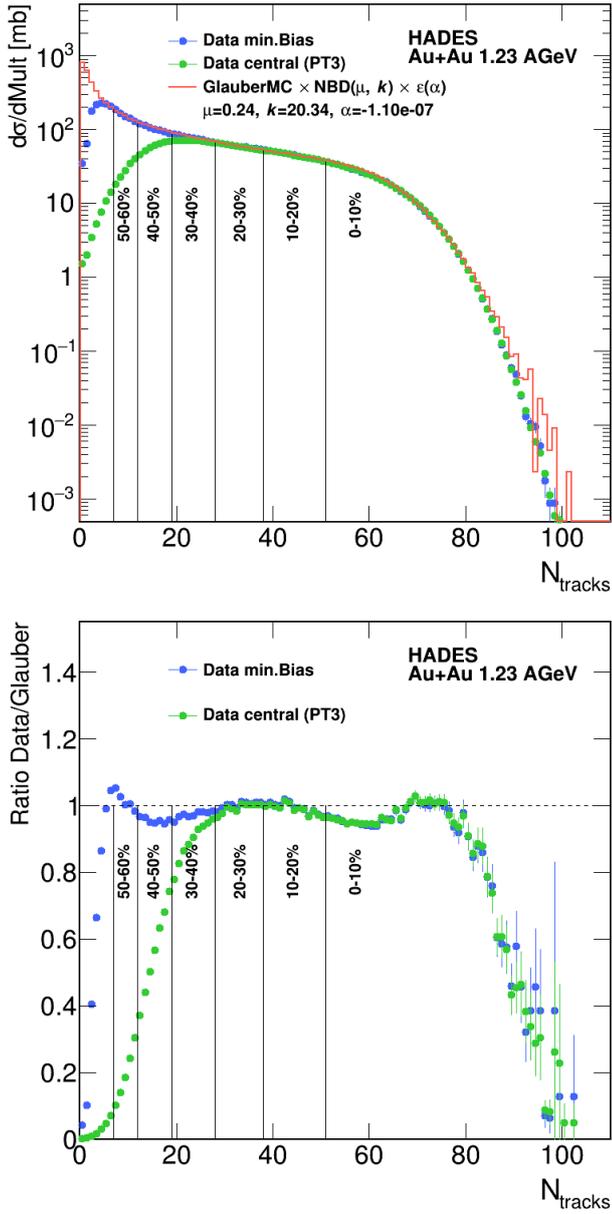
Fig. 2 Upper panel: The N_{tracks} distribution for minimum bias (blue symbols) and central (PT3 trigger, green symbols) data in comparison with a fit using the Glauber MC model (red histogram). The centrality classes are represented by the vertical lines. Lower panel: The ratio between data and the Glauber MC model.

Fig. 3 The $N_{hits}^{TOF+RPC}$ distributions for the sum of TOF and RPC hits. The upper panel shows minimum bias (blue symbols) and central (PT3 trigger, green symbols) data in comparison with the Glauber MC model (red histogram). The lower panel shows the same for a simulation based on minimum bias UrQMD events filtered through the detailed detector simulation (blue symbols) and in addition through an emulator of the PT3 trigger (green symbols).

Several triggers are implemented to start the data acquisition. The minimum bias trigger is defined by a signal in the START detector in the beam line (CVD diamond detector). In addition, online Physics Triggers (PT) are used, which are based on hardware thresholds on the TOF signals, proportional to the event multiplicity, corresponding to at least 5 (PT2) or 20 (PT3) hits in the TOF. Most physics analyses are based on the PT3 trigger, which covers the most central 43 % of the total cross section. Events are selected offline
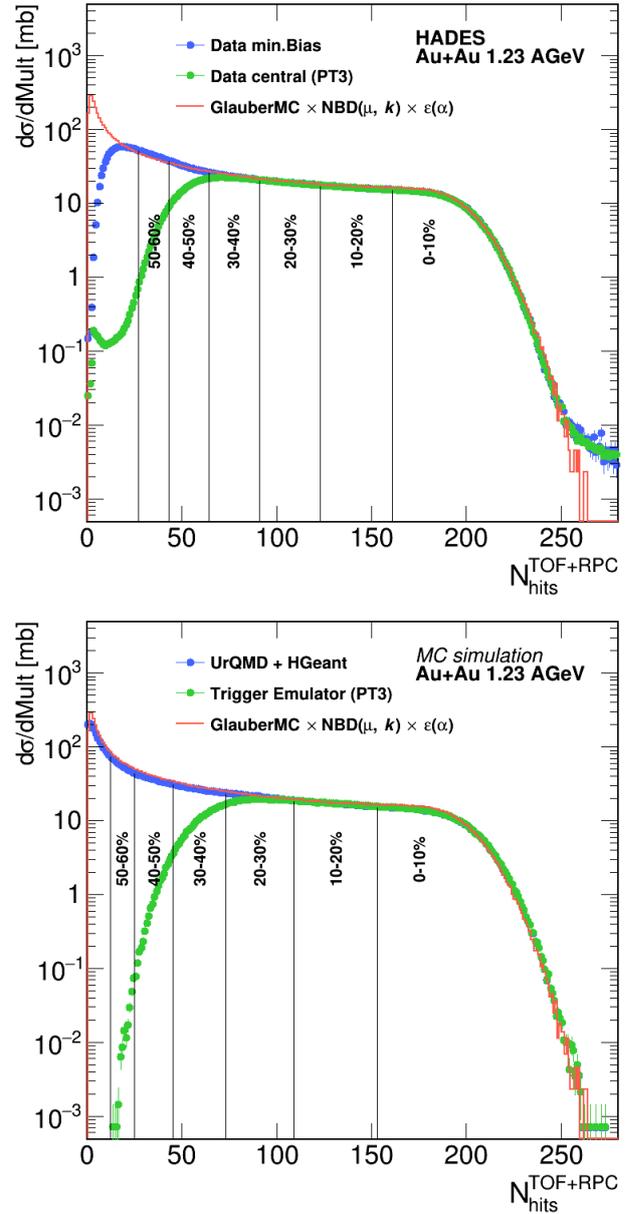
by requiring that their global event vertex is inside the target region, i.e. between $z = -65$ mm and 0 mm along the beam axis.

For the centrality determination currently two different experimental observables are considered within HADES, both of which provide a measurement of the charged particle density close to mid-rapidity. One is the number of tracks reconstructed with the MDCs N_{tracks}, while the other is based

on the summed number of hits detected by the TOF and the RPC detectors $N_{\mathrm{hits}}^{\mathrm{TOF+RPC}} = N_{\mathrm{hits}}^{\mathrm{TOF}} + N_{\mathrm{hits}}^{\mathrm{RPC}}$. The first has the advantage of being less contaminated by background hits, but requires a full reconstruction of the tracks in all MDCs. N_{tracks} contains only track candidates which do not share any space points with other tracks, who have a good matching of track to point position and have a distance-of-approach relative to the global event vertex of less than 10 mm. Since during the running period not all sectors of the MDC were always operational, we applied a time dependent correction to N_{tracks} in order to take these acceptance losses into account.

4 Centrality determination

Following the assumption of the wounded nucleon model, the measured charged particle multiplicity, N_{ch}, should on average be directly proportional to N_{part}. To allow for event-by-event fluctuations around this average value, N_{ch} for a given event is sampled from a Negative Binomial probability Distribution (NBD) with a mean μ, i.e.:

$$P_{\mu,k}(n) = \frac{\Gamma(n+k)}{\Gamma(n+1)\Gamma(k)} \cdot \frac{(\mu/k)^n}{(\mu/k+1)^{n+k}}, \qquad (5)$$

where Γ is the gamma function and the dispersion parameter k is related to the relative width by $\sigma/\mu = \sqrt{1/\mu + 1/k}$. On average, this procedure yields the proportionality $\langle N_{\mathrm{ch}} \rangle = \mu \cdot \langle N_{\mathrm{part}} \rangle$. The parameters μ and k take into account the acceptance, reconstruction efficiency and resolution of the specific observables ($N_{\mathrm{ch}} = N_{\mathrm{tracks}}$ or N_{hits}) and are determined by a minimization procedure in which the simulated N_{ch} distribution is fitted to the measured ones.

In order to take multiplicity dependent inefficiencies into account, the value sampled from the NBD is further folded with an efficiency function $\varepsilon(\alpha) = 1 - \alpha \cdot N_{\mathrm{part}}^2$. This function models the relative variation of the efficiency for charged tracks and parametrizes the corresponding efficiency obtained from events simulated with the transport model UrQMD [14] filtered through a detailed simulation of the detector response. Table 1 summarizes the parameters used for the different observables. Please note that for $N_{\mathrm{hits}}^{\mathrm{TOF+RPC}}$, the individual numbers $N_{\mathrm{hits}}^{\mathrm{TOF}}$ and $N_{\mathrm{hits}}^{\mathrm{RPC}}$ had to be fit separately, since the two measurements are subject to different systematic effects.

Observable	Parameter		
	μ	k	α
N_{tracks}	0.24	20.34	$1.10 \cdot 10^{-7}$
$N_{\mathrm{hits}}^{\mathrm{TOF}}$	0.20	6.36	$1.64 \cdot 10^{-6}$
$N_{\mathrm{hits}}^{\mathrm{RPC}}$	0.50	29.06	$1.64 \cdot 10^{-6}$

Table 1 The fit parameters obtained for the different observables.

The upper panel of Fig. 2 shows the comparison of the fit result to the measured N_{tracks} distribution. As illustrated
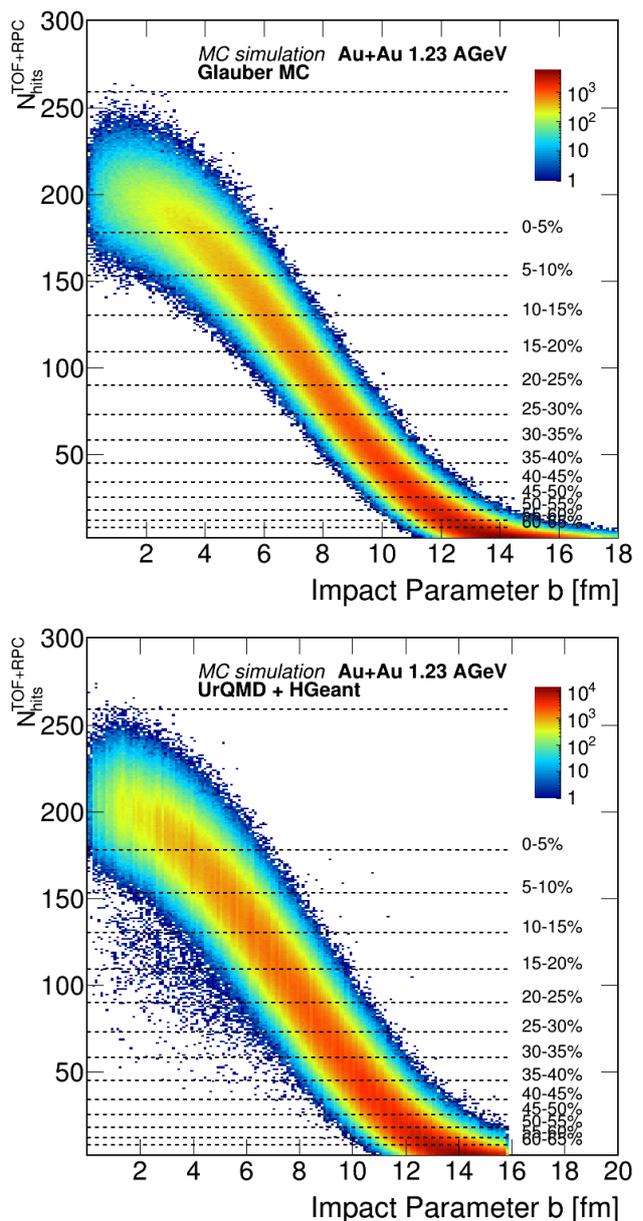

Fig. 4 The anti-correlation between the total number of hits $N_{\mathrm{hits}}^{\mathrm{TOF+RPC}}$ in TOF and RPC and the impact parameter b. The different centrality classes are indicated by the dashed lines. The upper panel is calculated with the Glauber MC model while the lower one is obtained from simulated UrQMD events.

by the ratio of data and fit result in the lower panel of the figure, a good description within ± 5 % is achieved for the 60 % most central part of the minimum bias data. Also, the largest part (i.e. most central 30 %) of the PT3 triggered events is fitted quite well. Below these centralities the corresponding trigger thresholds set in, which are not included in the Glauber MC model.

For the measured $N_{\mathrm{hits}}^{\mathrm{TOF+RPC}}$ distribution the comparison to the Glauber MC model is shown in the upper panel of Fig. 3.
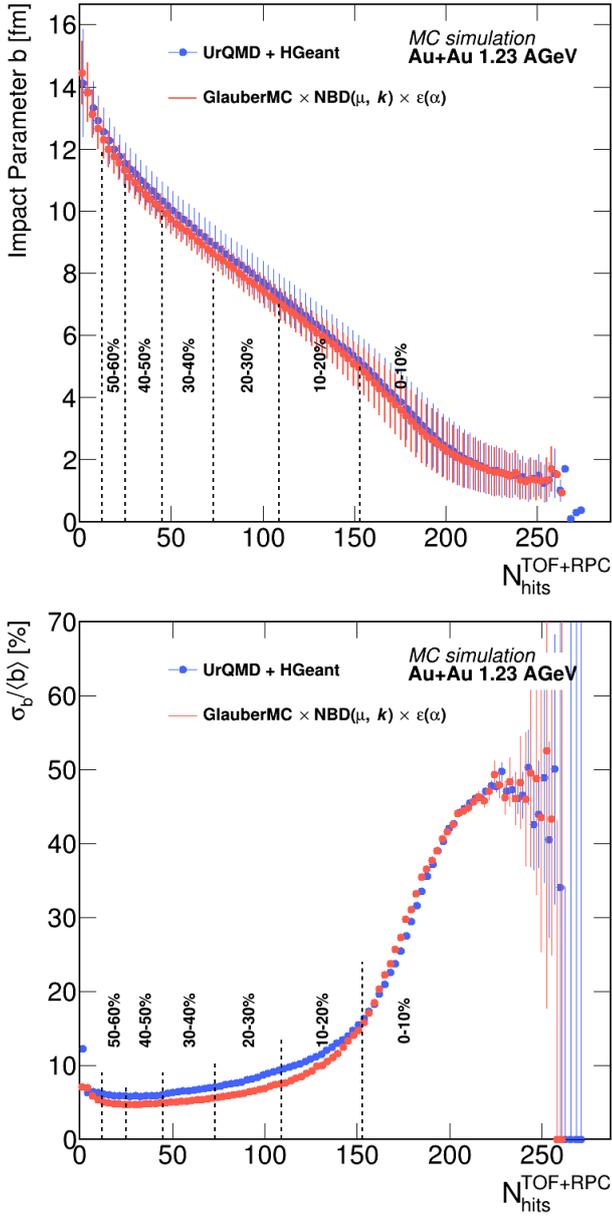
Fig. 5 Upper panel: The correlations between the impact parameter b and the total number of hits $N_{\text{hits}}^{\text{TOF+RPC}}$ in TOF and RPC, as obtained from simulated UrQMD events. The different centrality classes are indicated by the dashed lines. In one case b is taken directly from UrQMD (blue symbols), while in the other case (red symbols) it is derived from the Glauber MC model fit. The corresponding resolution in b, defined as the ratio of the Gaussian σ and the mean of the impact parameter distributions $\langle b \rangle$, is presented in the lower panel.

Fig. 6 Upper panel: The correlations between the impact parameter b and the total number of tracks N_{tracks}, as obtained from simulated UrQMD events. The different centrality classes are indicated by the vertical dashed lines. In one case b is taken directly from UrQMD (blue symbols), while in the other case (red symbols) it is derived from the Glauber MC model fit. The corresponding resolution in b, defined as the ratio of the Gaussian σ and the mean of the impact parameter distributions $\langle b \rangle$, is presented in the upper panel.

Also here a very good agreement is achieved in the same regions of the cross section. The fit has also been performed on UrQMD events, processed by the full detector simulation and reconstruction chain, as well as an additional emulator of the PT3 trigger (green symbols). As shown in the lower panel of Fig. 3, also the simulated data can be well described by the Glauber MC model fit, illustrating that our central-
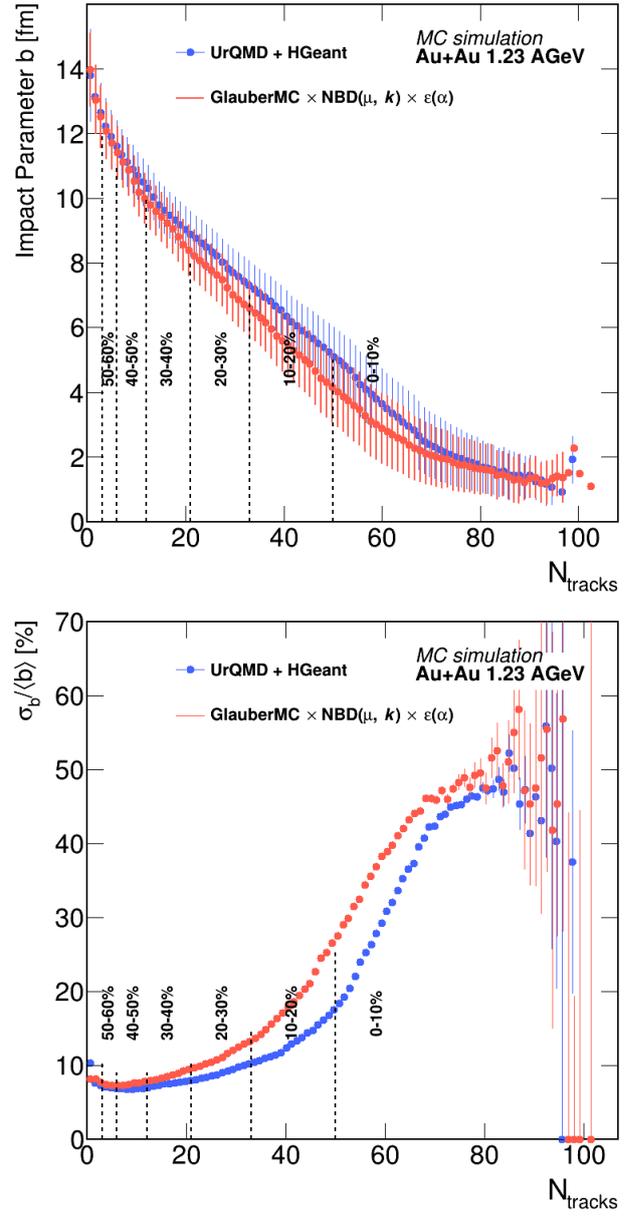
ity selection procedure provides a good correspondence between event classes defined in data and in models.

Centrality Classes	b_{min}	b_{max}	$\langle b \rangle$	$\langle N_{part} \rangle$	RMS(N_{part})	Uncertainties on $\langle N_{part} \rangle$		
						Model	$N_{hits}^{TOF+RPC}$	N_{tracks}
0 – 10 %	0.00	4.70	3.14	303.0	33.1	± 11.0	± 12.0	± 15.3
10 – 20 %	4.70	6.60	5.70	213.1	22.6	± 11.1	± 11.5	± 11.5
20 – 30 %	6.60	8.10	7.38	149.8	18.1	± 9.7	± 10.0	± 10.0
30 – 40 %	8.10	9.30	8.71	103.1	14.4	± 6.8	± 7.5	± 8.2
40 – 50 %	9.30	10.40	9.86	68.4	12.3	± 6.5	± 7.0	± 7.7

Table 2 Centrality classes in fixed intervals of impact parameter $b_{min} - b_{max}$ for Au+Au collisions at 1.23A GeV. Listed are the mean impact parameter $\langle b \rangle$, mean number of participants $\langle N_{part} \rangle$ and the RMS of the N_{part} distributions in the different centrality classes. Also given are the systematic uncertainties resulting from the variation of the Glauber model parameters as described in the text. The first corresponds to a centrality selection in the impact parameter, while in the case of the other two the fraction of the total cross section is selected from the observables $N_{hits}^{TOF+RPC}$ or N_{tracks} and thus also takes into account their different sensitivities in the centrality selection.

4.1 Systematic uncertainties

The systematic uncertainties on the $\langle N_{part} \rangle$ determination can be separated into two categories. On one side there are those related to the input parameters of the Glauber MC model itself, on the other side the different experimental centrality estimators introduce systematic deviations to the ideal model scenario.

To investigate systematic effects due to the model parameters, the fits were repeated with Glauber MC simulations based on different input parameters. The inelastic nucleon-nucleon cross section was varied up to $\sigma_{inel}^{NN} = 30$ mb, which causes a change of the extracted $\langle N_{part} \rangle$ values of around 5 %, almost independent of centrality. As different parameters for the radial charge density distribution, the values $R = 6.75$ fm and $a = 0.623$ fm, as well as $R = 6.35$ fm and $a = 0.423$ fm, were used, motivated by [15] and [16], respectively. In comparison to the default parameter selection this causes a variation of $\langle N_{part} \rangle$ of at most 15 % for very peripheral collisions, which decreases to 3 – 4 % for very central ones. Furthermore, the fits were repeated with an inter-nucleon exclusion distance of $d_{min} = 0$. It was found that this modification affects the resulting $\langle N_{part} \rangle$ by not more than 3 %. The final systematic uncertainty of $\langle N_{part} \rangle$ from the Glauber MC model is determined as the maximal deviation between the different parameter sets and procedures to the default version for each centrality.

While the above discussed systematic effects are inherent of the ideal geometrical Glauber MC model implementation, additional effects have to be taken into account for the experimental centrality estimators. On one side these are due to different levels of background and distortions, which cause deviations from the ideal multiplicity estimation. On the other side the estimators provide different resolutions for the event centrality due to the reconstructed event-wise multiplicities (N_{tracks} is on average smaller than $N_{hits}^{TOF+RPC}$, because of the more stringent cuts). Therefore, $\langle N_{part} \rangle$ was calculated again according to the corresponding fraction of the total cross section as determined by $N_{hits}^{TOF+RPC}$, respectively N_{tracks}, instead of using cuts on the impact parameter. It is found that the resulting $\langle N_{part} \rangle$ differs by less than 1 % in the case of

$N_{hits}^{TOF+RPC}$ from the value given in Tab. 2. For N_{tracks} a slightly larger deviation of 3 % is observed for the 10 % most central events, while it is 1 % in the other centrality ranges.

4.2 Centrality classes

The above described Glauber MC model implementation results in a total cross section for Au+Au collisions at 1.23A GeV of $\sigma_{tot}^{Au+Au} = (6833 \pm 430)$ mb. The events can thus be categorized into centrality classes according to their fraction of σ_{tot}^{Au+Au}. Using the fits shown in Figs. 2 and 3 this can be translated into intervals of N_{tracks}, respectively $N_{hits}^{TOF+RPC}$, corresponding to these centrality classes. Figure 4 shows the anti-correlation of $N_{hits}^{TOF+RPC}$ and the impact parameter b, obtained from the Glauber MC model (upper panel) and from simulated UrQMD events (upper panel). Over a large part of the total cross section a well defined anti-correlation is visible in both, allowing a good separation of the different centrality classes, here indicated by the dashed lines. As illustrated in the upper panel of Fig. 5, these two anti-correlations are in very good agreement. This demonstrates that a meaningful comparison of centrality selected events is possible between data and model using $N_{hits}^{TOF+RPC}$. From these anti-correlations also the resolution in the impact parameter can be derived (see upper panel of Fig. 5). It is here defined as the ratio of the dispersion σ obtained with a Gaussian fit to the mean of the corresponding b distribution at a given $N_{hits}^{TOF+RPC}$. Also here, a reasonable agreement is achieved between UrQMD and the Glauber MC model fit. The resolution is found to be below 15 % for all centralities, except for the very central interval $0 - 5$ %. Figure 6 shows the same comparison for the observable N_{tracks}.

The distributions of the impact parameter b and number of participants N_{part} for different centrality classes, as selected by $N_{hits}^{TOF+RPC}$, are shown in Fig. 7. The averaged values are summarized in Tab. 2. Even though the distributions have some overlap (the corresponding RMS values can also be found in Tab. 2), a clear separation of the centrality classes is possible.
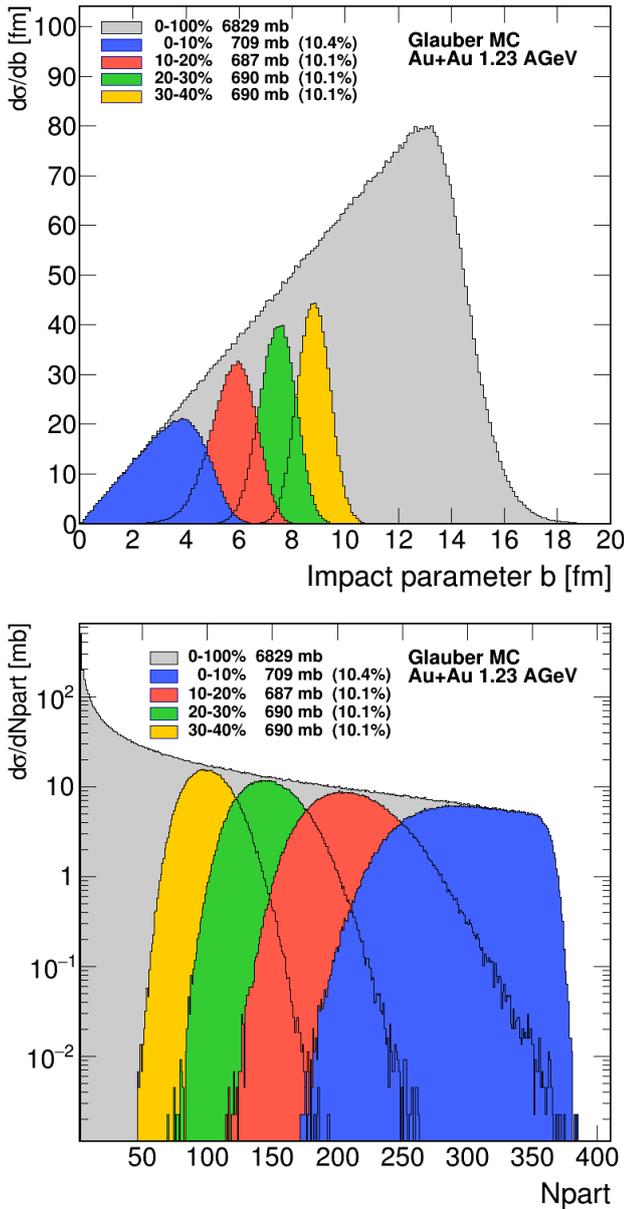
Fig. 7 Upper panel: the distributions of the impact parameter b calculated with the Glauber MC model. The colored distributions represent the four most central centrality classes selected by the number of hits in the TOF and RPC detectors $N_{\mathrm{hits}}^{\mathrm{TOF+RPC}}$. Upper panel: the corresponding distributions of the number of participants N_{part}.

5 Conclusions

The Glauber Monte Carlo model has been employed for the event characterization of Au+Au collisions at $1.23A$ GeV, as measured with HADES at the GSI-SIS18. The different experimental centrality estimators, number of reconstructed tracks, N_{tracks}, and number of recorded hits in TOF and RPC, $N_{\mathrm{hits}}^{\mathrm{TOF+RPC}}$, can successfully be described by the model fits. Based on these fits the events can thus be selected in different centrality classes with corresponding average number of participating nucleons $\langle N_{\mathrm{part}} \rangle$ and impact parameter $\langle b \rangle$.

References

1. Glauber R J 1955 *Phys. Rev.* **100** 242–248
2. Glauber R J 1959 *Lectures in Theoretical Physics* vol 1 (Interscience, New York) p 315
3. Glauber R J 2006 *Nucl. Phys.* **A774** 3–13 (*Preprint* nucl-th/0604021)
4. Miller M L, Reygers K, Sanders S J and Steinberg P 2007 *Ann. Rev. Nucl. Part. Sci.* **57** 205–243 (*Preprint* nucl-ex/0701025)
5. Abelev B *et al.* (ALICE) 2013 *Phys. Rev.* **C88** 044909 (*Preprint* 1301.4361)
6. Bialas A, Bleszynski M and Czyz W 1976 *Nucl. Phys.* **B111** 461
7. Buuck M and Miller G A 2014 *Phys. Rev.* **C90** 024606 (*Preprint* 1406.2264)
8. Loizides C, Nagle J and Steinberg P 2014 (*Preprint* 1408.2549)
9. Kardan B 2015 *Centrality Determination at 1.23 AGeV Gold-Gold Collisions and Readout-Electronics for the HADES Calorimeter* Diploma-thesis Goethe-Universität Frankfurt am Main
10. Fricke G and Heilig K 2004 *Nuclear Charge Radii* (*Landolt-Börnstein - Group I Elementary Particles, Nuclei and Atoms* vol 20) (Springer Berlin Heidelberg) pp 1 – 4
11. Olive K A *et al.* (Particle Data Group) 2014 *Chin. Phys.* **C38** 090001
12. Bystricky J, La France P, Lehar F, Perrot F, Siemiarczuk T and Winternitz P 1987 *J. Phys. France* **48** 1901–1924
13. Agakishiev G *et al.* (HADES) 2009 *Eur. Phys. J.* **A41** 243–277 (*Preprint* 0902.3478)
14. Bass S A *et al.* 1998 *Prog. Part. Nucl. Phys.* **41** 255–369 [Prog. Part. Nucl. Phys.41,225(1998)] (*Preprint* nucl-th/9803035)
15. Hahn B, Ravenhall D G and Hofstadter R 1956 *Phys. Rev.* **101** 1131–1142
16. Buss O, Gaitanos T, Gallmeister K, van Hees H, Kaskulov M, Lalakulich O, Larionov A B, Leitner T, Weil J and Mosel U 2012 *Phys. Rept.* **512** 1–124 (*Preprint* 1106.1344)